

Electronic Supplementary Information (ESI)

Dicopper(II) paddle-wheel metal-organic frameworks for high propyne storage under ambient conditions

Xing-Ping Fu,^{1,2} Ji-Wei Shen,¹ Ling Chen,^{*1} De-Xin Zhong,¹ Yu-Ling Wang^{*1} and Qing-Yan Liu^{*1}

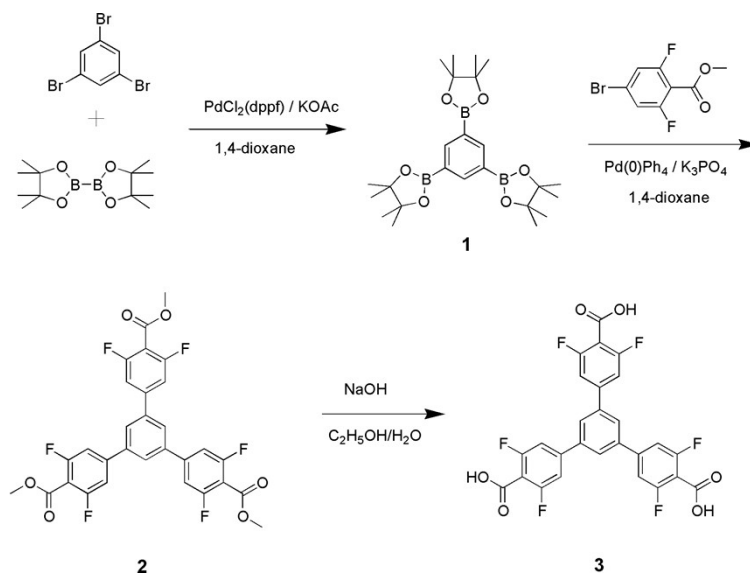
¹ College of Chemistry and Chemical Engineering, Key Lab of Fluorine and Silicon for Energy Materials and Chemistry of Ministry of Education, Jiangxi Normal University, Nanchang 330022, Jiangxi, P. R. China. ² Department of Ecological and Resources Engineering, Fujian Key Laboratory of Eco-industrial Green Technology, Wuyi University, Wuyishan 354300, Fujian, P. R. China.

General Methods and Materials

All chemicals were obtained from commercial sources and used without further purification except 1,3,5-tri(3,5-bifluoro-4-carboxyphenyl)benzene, which was prepared as Scheme S1. Unless otherwise noted, all the reactions were performed under air without an inert atmosphere. The powder X-ray diffraction patterns (PXRD) were recorded on a Rigaku DMAX 2500 powder diffractometer (Cu-K α , $\lambda=1.54056$ Å). FT-IR spectrum was recorded on a Perkin-Elmer Spectrum One FT-IR spectrometer. Thermogravimetric analyses were performed under a nitrogen atmosphere with a heating rate of 10 °C min⁻¹ using a PE Diamond thermogravimetric analyzer. ¹H nuclear magnetic resonance spectra were recorded with a Bruker AVANCE 400 spectrometer. The C, H and N analyses were performed on Elementar Perkin-Elmer 2400CHN microanalyzer.

Synthesis of 1,3,5-tri(3,5-bifluoro-4-carboxyphenyl)benzene (H₃-SFBTB) ligand.

1,3,5-Tribromobenzene (6.00 g, 19.0 mmol), bis(pinacolato)diboron (21.72 g, 85.5 mmol) and potassium acetate (16.76 g, 171.0 mmol) were added into anhydrous 1,4-dioxane (500 mL). After purging the system with N₂ for 30 min, Pd(dppf)Cl₂ (0.83 g, 1.14 mmol) was added quickly and N₂ was purged through the mixture for another 30 min. The suspension was then heated at 110 °C under N₂ for 3 days. After cooling down to room temperature, the resulting mixture was filtrated. The filtrate was removed under reduced pressure and the residues was purified by column chromatography to afford **1** as white solid (8.06 g, 93% yield). ¹H NMR (400 MHz, CDCl₃), δ 8.36 (s, 3H) and 1.33 (s, 36H).



Scheme S1. Synthesis of 1,3,5-tri(3,5-bifluoro-4-carboxyphenyl)benzene (H_3SFBTB) ligand.

Solution of **1** (4.56 g, 10.0 mmol) and methyl 4-bromo-2,6-difluorobenzoate (8.28 g, 33.0 mmol) in 1,4-dioxane (300 mL) was degassed by bubbling nitrogen for 30 minutes. Then, $\text{Pd}(0)\text{Ph}_4$ (0.88 g, 1.2 mmol) and finely grounded potassium phosphate tribasic (19.1 g, 90.0 mmol) were added into the solution quickly. The resulting mixture was stirred at 110 °C for 3 days under nitrogen atmosphere. After cooling down to room temperature, the final resulting mixture was filtrated. The filtrate was concentrated under reduced pressure and the residues was subjected to column chromatography to yield **2** as yellow solid (5.11 g, 86.7% yield). ^1H NMR (400 MHz, CDCl_3), δ 7.76 (s, 3H), 7.28 (d, $J = 8.6$ Hz, 6H), and 4.00 (s, 9H).

Compound **2** (5.00 g, 8.5 mmol) was suspended in 100 mL of THF, to which 100 mL of 2 M NaOH aqueous solution was added. The suspension was heated and stirred for 24 h before the solvent was removed by rotary evaporation. The residues were dissolved in water and acidified with 1 M HCl to yield 1,3,5-tri(3,5-bifluoro-4-carboxyphenyl)benzene as yellow precipitate. After dried under high vacuum, 1,3,5-tri(3,5-bifluoro-4-carboxyphenyl)benzene was obtained as yellow solid (4.50 g, 96% yield). ^1H NMR (400 MHz, $\text{DMSO}-d_6$), δ 12.93 (s, 3H), 8.22 (s, 3H), and 7.95 (d, $J = 9.6$ Hz, 6H).

Synthesis of $[\text{Cu}_2(\text{SFBTB})_{4/3}(\text{BPY})]_n$ (JXNU-16F).

$\text{Cu}(\text{NO}_3)_2 \cdot 3\text{H}_2\text{O}$ (0.08 mmol), 1,3,5-tri(3,5-bifluoro-4-carboxyphenyl)benzene (0.02 mmol), 4,4'-bipyridine (0.03 mmol), and trifluoroacetic acid (0.10 mL) were mixed with 1.5 mL N,N-

dimethylformamide (DMF) and 1.5 mL CH₃CH₂OH. The mixture was ultrasonicated for 10 min under room temperature and then transferred into a 20 mL vial, which was heated in an oven at 100 °C for 24 hours. Blue polyhedral-shaped crystals were generated after cooling to room temperature (yield 58%). Elemental analysis for {[Cu₂(SFBTB)_{4/3}(BPY)]·4DMF·5H₂O}_n (1390.18). (calc/found: C, 50.11/50.56; H, 4.20/4.02; N, 6.04/6.08). IR data (KBr, cm⁻¹): 3432 (s), 2933 (w), 1631 (s), 1391 (s), 1221 (w), 1104 (w), 1032 (s), 844 (m), 814 (w), 706 (w), 592 (m), 408 (m).

Synthesis of [Cu₂(BTB)_{4/3}(BPY)]_n (JXNU-16).

Cu(NO₃)₂·3H₂O (0.08 mmol), 1,3,5-tri(4-carboxyphenyl)benzene (0.02 mmol), 4,4'-bipyridine (0.03 mmol), and trifluoroacetic acid (0.15 mL) were mixed with 1.5 mL N,N-dimethylformamide (DMF) and 1.5 mL CH₃CH₂OH. The mixture was ultrasonicated for 10 min under room temperature and then transferred into a 20 mL vial, which was heated in an oven at 100 °C for 24 hour. Blue polyhedral-shaped crystals were generated after cooling to room temperature (yield 52%). Elemental analysis for {[Cu₂(BTB)_{4/3}(BPY)]·4DMF·3.5H₂O}_n (1219.24). (calc/found: C, 57.13/57.02; H, 5.21/5.11; N, 6.89/6.81). IR data (KBr, cm⁻¹): 3446 (s), 2939 (w), 1632 (s), 1397 (s), 1192 (w), 1035 (s), 846 (m), 814 (w), 706 (w), 600 (m), 411 (m).

X-Ray Single Crystal Structure Determinations.

Single-crystal X-ray diffraction experiments were carried out with a Rigaku Oxford SuperNova diffractometer equipped with an EOS detector (Mo-K α radiation, $\lambda = 0.71073$ Å). Absorption correction and data reduction were handled with a *CrysAlisPro package*.^[S1] The *SHELXT-2015*^[S2] and *SHELXL-2018*^[S3] were applied to structure solution and refinement. Non-H atoms were refined anisotropically. Hydrogen atoms were modelled geometrically and refined with a riding model. The aromatic rings of the organic ligands were disordered over two positions. The guest solvent molecules are highly disordered and treated by *SQUEEZE* of *PLATON*.^[S4] The crystallographic data are provided in Table S1.

Gas Adsorption

Gas sorption-desorption isotherms were measured on a Micromeritics ASAP 2020 HD88 surface-area. N₂ (99.99%) and C₃H₄ (99.95%) were purchased and directly used. The Brunauer-Emmett-

Teller (BET) surface area and the pore size distribution data was calculated from N₂ adsorption isotherms at 77 K. The as-synthesized samples were washed with DMF several times, then ethanol-exchanged for 3 days and *n*-hexane-exchanged for 2 days at room temperature. The activated samples were obtained under a dynamic vacuum at 60 °C for 10 h.

Isosteric Analysis of the Heat of Adsorption.

The gas adsorption isotherms measured at 273, 285, and 298 K were first fitted to a virial equation (eqn (S1)). Then the Q_{st} values for C₃H₄ was calculated based on the fitting parameters using eqn (S2).^[S5]

$$\ln P = \ln N + \frac{1}{T} \sum_{i=0}^m a_i N^i + \sum_{i=0}^n b_i N^i \quad \text{eqn (S1)}$$

$$Q_{st} = -R \sum_{i=0}^m a_i N^i \quad \text{eqn (S2)}$$

where P is pressure (mmHg), N is the adsorbed quantity (mmol g⁻¹), T is the temperature (K), a_i and b_i are virial coefficients, R is the universal gas constant (8.314 J K⁻¹ mol⁻¹), and m and n determine the number of coefficients required to adequately describe the isotherm.

Grand canonical Monte Carlo (GCMC) simulation.

All GCMC simulation was performed using the Materials Studio 5.5 package. The adsorption properties of C₃H₄ were obtained from GCMC simulations in the Sorption module. The host framework and the guest molecules were both regarded as rigid. The simulation box consisted of eight unit cell and the Metropolis method based on the universal forcefield (UFF) was used. The Q_{Eq} derived charges and the ESP charges derived by DFT were employed to the host framework and guest atoms, respectively. The cutoff radius was chosen as 15.5 Å for the Lennard-Jones (LJ) potential, and the equilibration steps and production steps were both set as 5×10^6 . To obtain the gas binding energy, a gas molecule placed in a supercell with the same cell dimensions was also relaxed as a reference. The static binding energy (at $T = 0$ K) was then calculated using $E_B = E_{(JXNU-16F)} + E_{(gas\ molecule)} - E_{(JXNU-16F + gas\ molecule)}$.

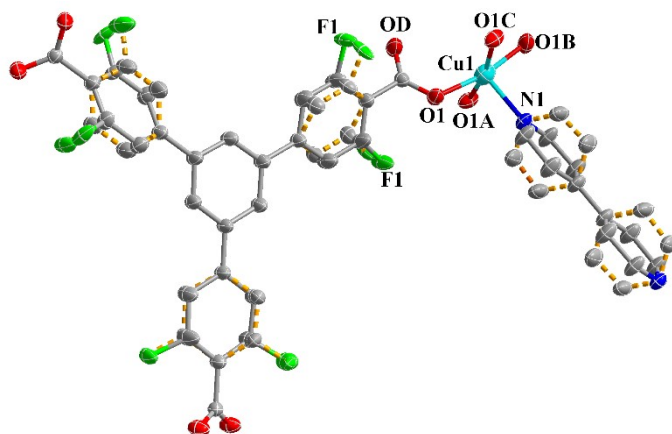


Fig. S1 Coordination environments for Cu(II) atoms in JXNU-16F with displacement ellipsoids of 30% probability level.

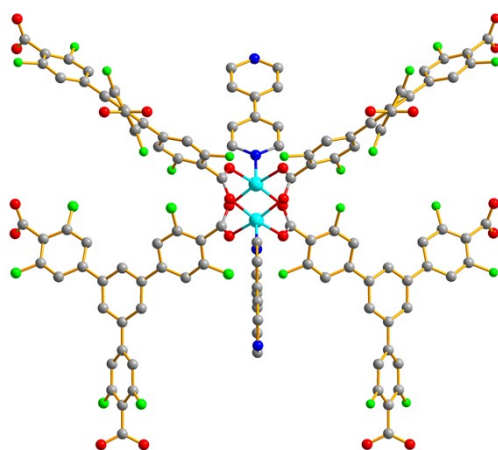


Fig. S2 The Cu(II) paddle-wheel is surrounded by four SFBTB³⁻ and two 4,4'-bipyridine ligands in JXNU-16F.

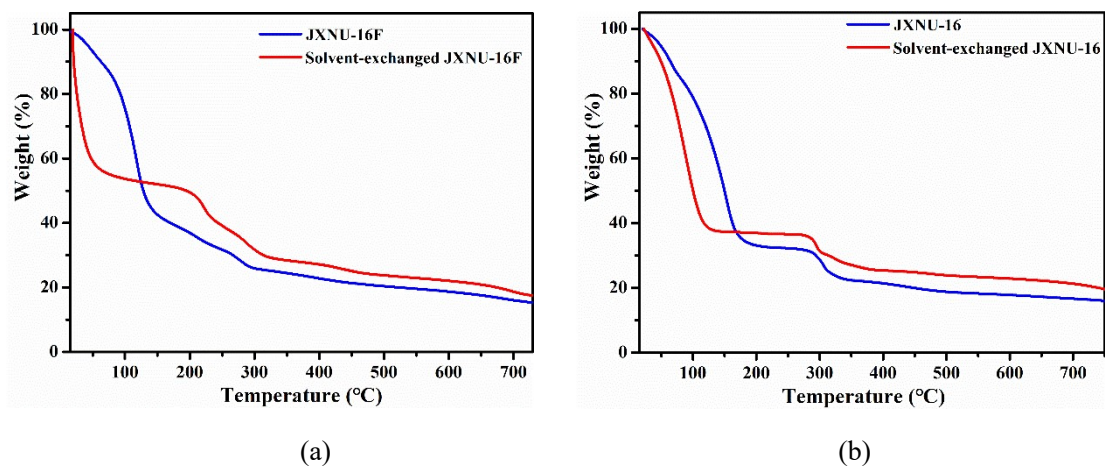


Fig. S3 TGA curves for JXNU-16F (a) and JXNU-16.

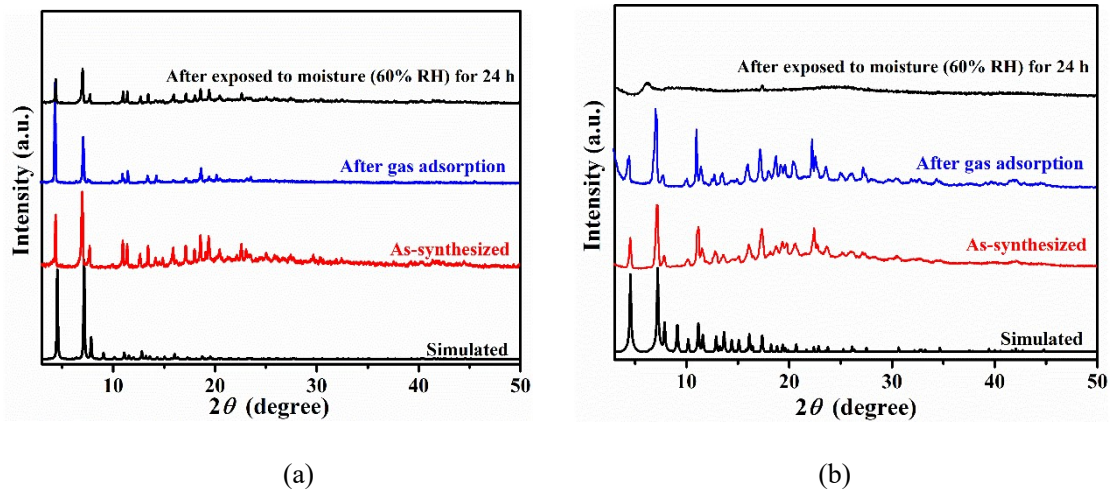


Fig. S4 PXRD patterns for (a) JXNU-16F and (b) JXNU-16. Slightly broadening of the peaks were observed in the PXRD patterns of the samples of JXNU-16 after gas adsorption, which is associated with the presence of an amorphous phase.

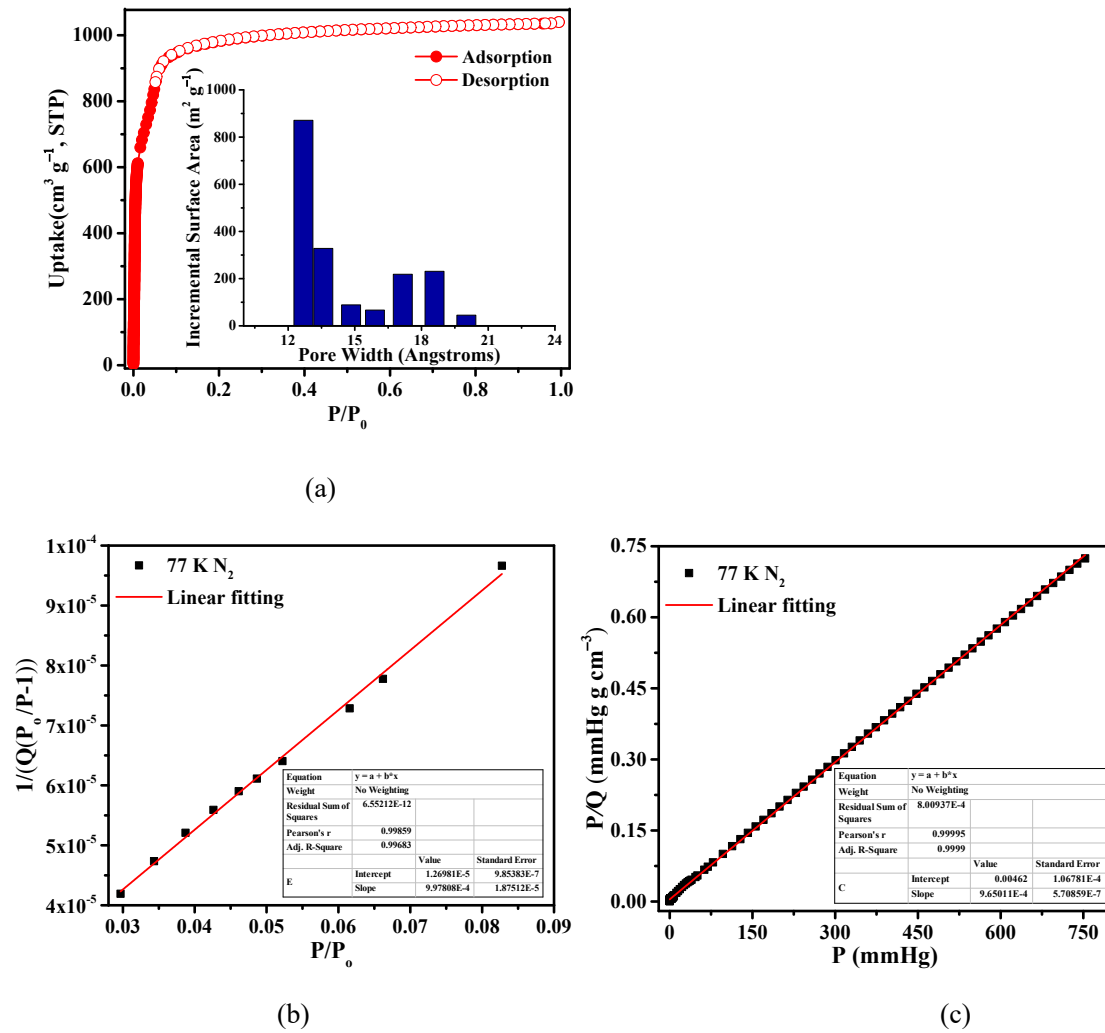


Fig. S5 (a) N_2 adsorption isotherms (77 K) for JXNU-16F (Inset: pore size distribution obtained using the non-localized density functional theory method), (b) BET surface area plots and (c) Langmuir surface area plots of JXNU-16F.

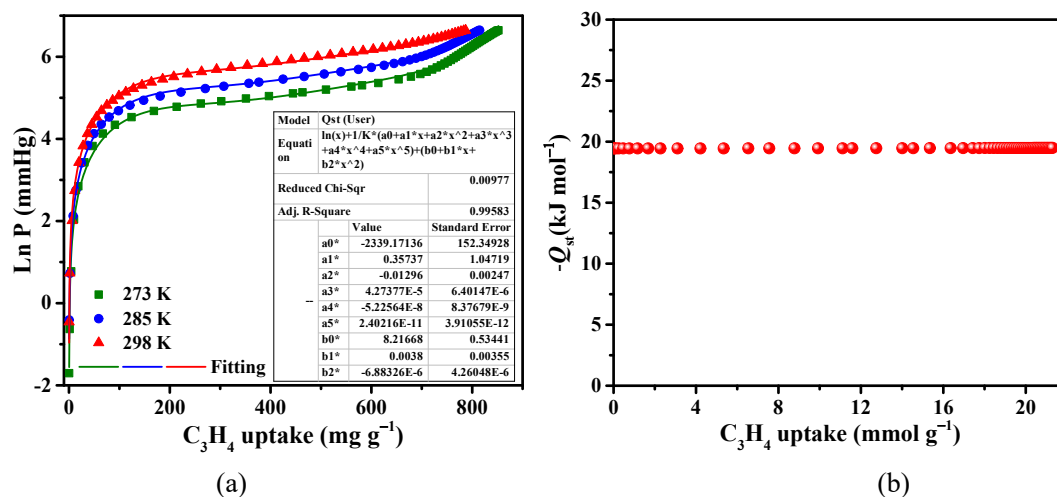


Fig. S6 (a) Fits of C_3H_4 isotherms with Virial equation S1 and (b) the Q_{st} for C_3H_4 in JXNU-16F.

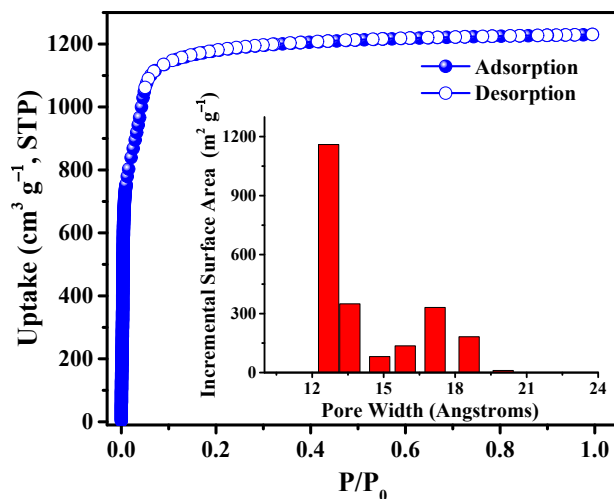


Fig. S7 N_2 adsorption isotherms (77 K) for JXNU-16 (Inset: pore size distribution obtained using the non-localized density functional theory method).

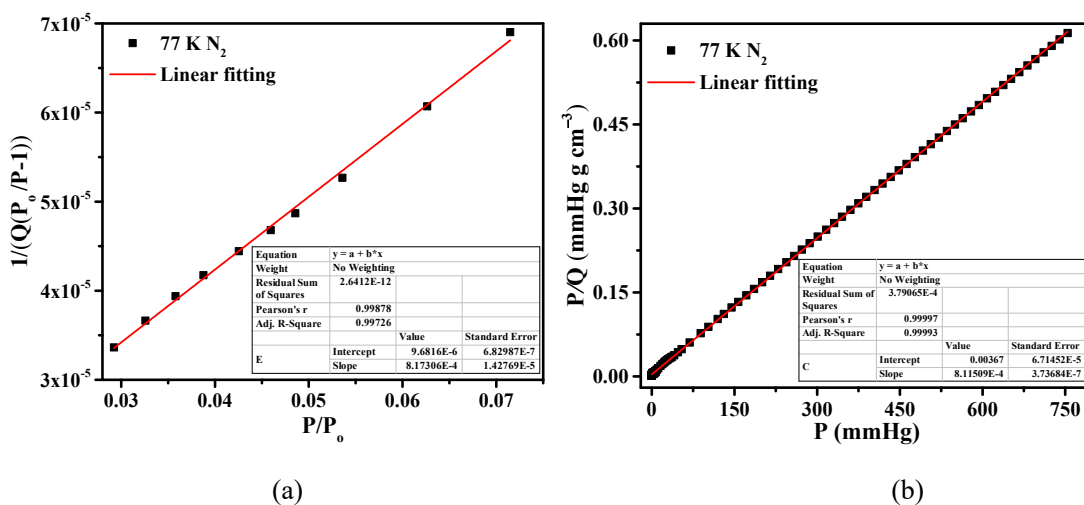


Fig. S8 (a) BET surface area plots and (b) Langmuir surface area plots of JXNU-16.

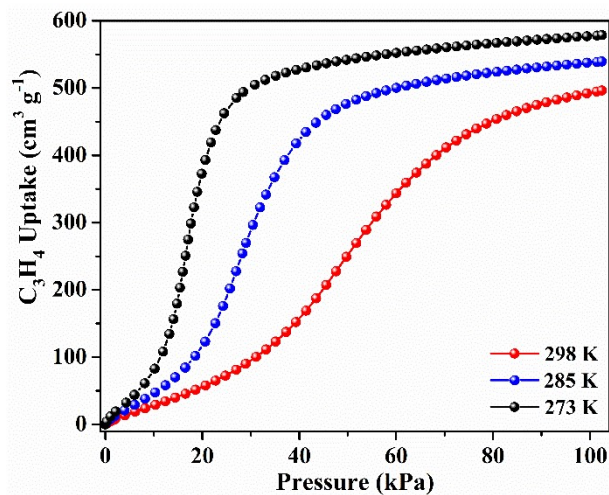


Fig. S9 C_3H_4 gravimetric adsorption isotherms for JXNU-16.

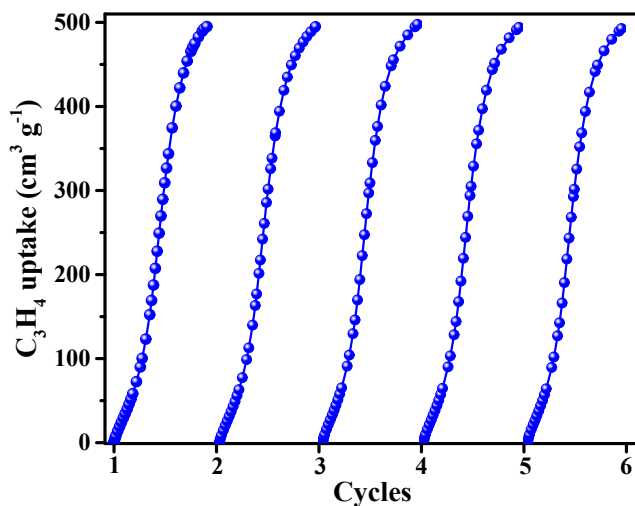


Fig. S10 Cycles of C_3H_4 gravimetric adsorption for JXNU-16 at 298 K and 1 atm.

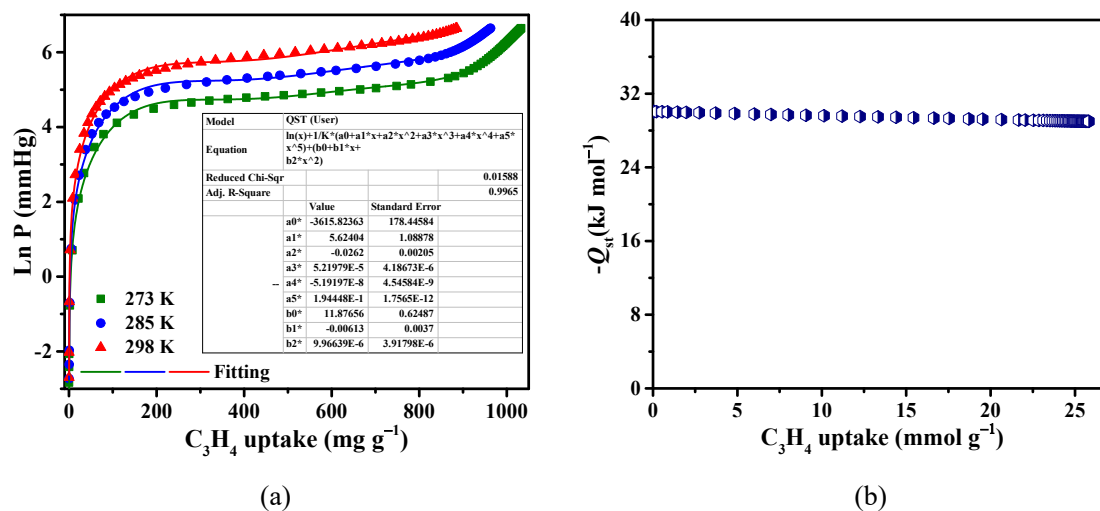


Fig. S11 (a) Fits of C_3H_4 isotherms with Virial equation S1 and (b) the Q_{st} for C_3H_4 in JXNU-16.

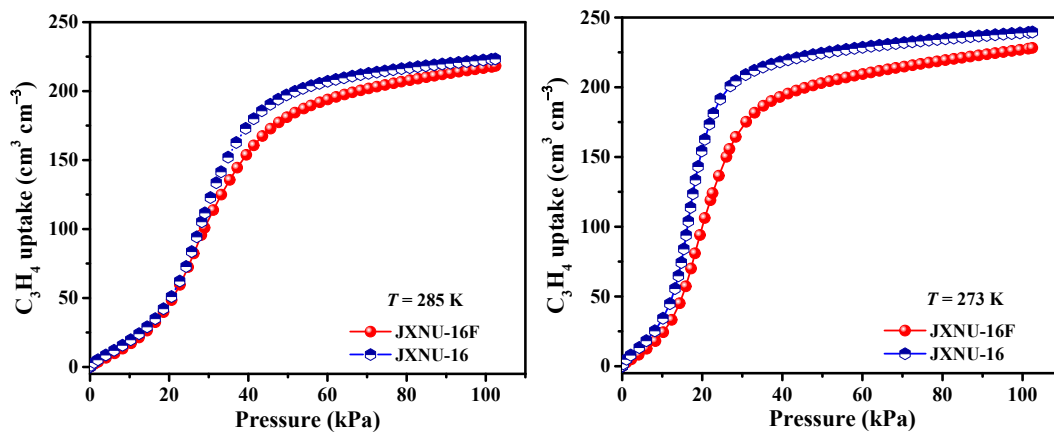


Fig. S12 Comparison of C_3H_4 volumetric adsorption isotherms of JXNU-16F and JXNU-16.

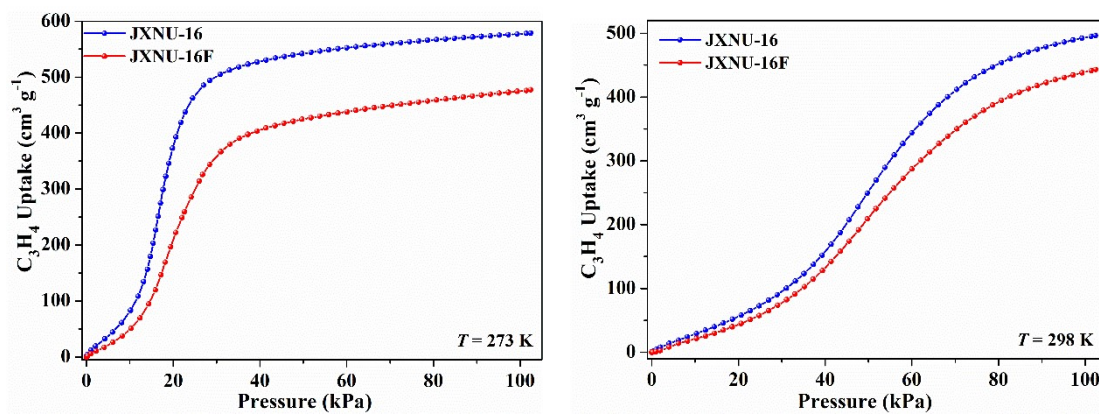


Fig. S13 Comparison of C_3H_4 gravimetric adsorption isotherms of JXNU-16F and JXNU-16.

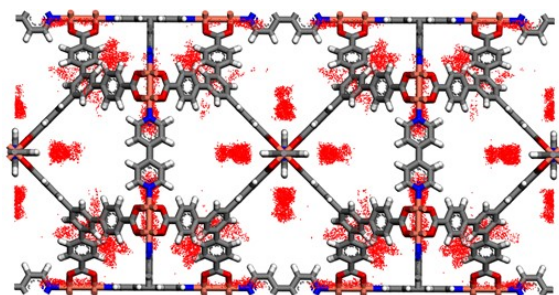


Fig. S14 Density distribution contours of C_3H_4 in JXNU-16 at 298 K and 1 atm obtained from GCMC simulation.

Table S1 Crystal structure refinement data.

JXNU-16F	
Empirical formula	C ₅₈ H ₅₈ F ₈ N ₆ O ₁₇ Cu ₂
Formula weight	1390.18
Temperature	293(2) K
Wavelength	0.71073 Å
Crystal system	cubic
space group	<i>Pmn</i>
<i>a</i> (Å)	27.5946(3)
<i>b</i> (Å)	27.5946(3)
<i>c</i> (Å)	27.5946(3)
α (°)	90
β (°)	90
γ (°)	90
Volume(Å ³)	21012.7(7)
<i>Z</i>	6
Calculated density(g cm ⁻³)	0.659
<i>F</i> (000)	4284
Limiting indices	-10 ≤ <i>h</i> ≤ 31, -20 ≤ <i>k</i> ≤ 25, -34 ≤ <i>l</i> ≤ 18
Reflections collected	19530
Independent reflections	3815 [<i>R</i> _{int} = 0.0412]
Goodness-of-fit on <i>F</i> ²	1.052
Final <i>R</i> ₁ [<i>I</i> > 2σ(<i>I</i>)]	0.0590
<i>wR</i> ₂ (all data)	0.2005
CCDC number	2216657

Table S2 Comparison of surface area (*S*_{BET}), pore volume, crystal density, thermal stability (Temperature for collapse of framework), and gravimetric and volumetric propyne adsorption capacity (298 K and 1 atm) for reported MOFs.

MOFs	<i>S</i> _{BET} (m ² g ⁻¹)	Pore volume (cm ³ g ⁻¹)	crystal density (g cm ⁻³)	thermal Stability (°C)	C ₃ H ₄ uptake (cm ³ cm ⁻³)	C ₃ H ₄ uptake (cm ³ g ⁻¹)	Ref.
MIL-100(Fe)	2800	—	0.69	270	281	384	S6
MIL-100(Cr)	3100	1.16	0.732	240	238	325	S6
Fe-BTT	2200	0.715	0.797	180	210	278	S6
UIO-66	1390	—	1.198	450	175	229	S6
Mg-MOF-74	1415	—	0.92	—	194	211	S6
Fe-MOF-74	1360	—	1.126	—	200	175	S6
Co-MOF-74	1080	—	1.169	—	196	170	S6

UTSA-74-Zn	830	0.39	1.34	260	223	166	S6
Cr-BTT	2293	—	0.832	—	123	163	S6
ZIF-8	1630	0.663	1.067	550	150	140	S6
Ni-MOF-74	1070	—	1.203	—	149	123	S6
UTSA-100	970	0.399	1.146	150	137	120	S6
ZJUT-1	222	0.15	1.738	—	87	51.2	S6
UTSA-200	612	0.27	1.417	—	114	80.2	S6
Th-TFBPDC	865	0.70	1.047	310	191.4	182.8	S7
JXNU-6	865	0.38	1.213	360	138.0	113.6	S8
Mg-Gallate	559	0.23	1.411	—	118.5	84.0	S9
Co-Gallate	475	0.20	1.536	240	110.4	71.9	S9
Ni-Gallate	424	0.18	1.589	290	94.3	59.4	S9
GeFSIX-dps-Cu	382	0.183	1.352	233	112	82.9	S10
ZU-62	476	0.30	1.378	230	112.3	82	S11
NKMOF-1-Ni	420	0.245	1.713	—	134.3	78.4	S12
NKMOF-1-Cu	382	0.218	1.734	—	128.2	73.9	S12
Ca-based MOF	224	0.12	1.938	500	130.6	67.4	S13
SIFSIX-3-Ni	250	0.167	1.57	—	100	64	S14
SIFSIX-2-Cu-i	735	—	1.247	—	105	84	S14
SIFSIX-1-Cu	1178	0.683	0.864	—	167	196.2	S14
ELM-12	740	0.141	1.406	—	57	62	S15
ZU-33	—	—	1.492	460	120	81	S16
HKUST-1	1850	—	0.879	240	206	235	S17
MOF-505	1830	—	0.992	—	244	246	S17
MIL-101(Cr)	4100	—	—	320	—	285	S17
ZNU-2	1380	0.575	1.02	440	176	172	S18
ZU-13	481	—	1.332	240	116	87	S19
APPT-Cd-MOF	—	—	1.538	320	67.4	43.8	S20
Cu-INA	428.7	0.284	1.589	250	98.5	62	S21
Cu-FINA-1	389.4	0.245	1.703	260	68.6	40.3	S21
Cu-FINA-2	175.9	0.097	1.662	260	50.7	30.5	S21
ZU-16-Co	—	0.109	1.61	—	95.8	59.4	S22
NKMOF-11	376	0.158	1.713	—	119	69.4	S23
FJI-W1	1376	0.54	0.898	200	142	159	S24
BUT-306	305	—	1.345	—	39.8	29.6	S25
BUT-310	1811	—	0.676	170	164	243	S26
JXNU-16	5263	1.91	0.414	200	205	496	
JXNU-16F	4308	1.61	0.478	240	211	443	

“—” indicates the data not available.

Table S3 Comparison of N₂ gas uptake (77 K), surface area, total pore volume and C₃H₄ uptake (298 K and 1 atm) of JXNU-16 and JXNU-16F.

MOFs	N ₂ uptake (cm ³ g ⁻¹)	S _{BET} (m ² g ⁻¹)	pore volume (cm ³ g ⁻¹)	C ₃ H ₄ uptake (cm ³ cm ⁻³)	C ₃ H ₄ uptake (cm ³ g ⁻¹)
JXNU-16	1230	5263	1.91	205	496
JXNU-16F	1040	4308	1.61	211	443

References

- 1 *CrysAlisPro*, Rigaku Oxford Diffraction: The Woodlands, TX. 2015.
- 2 G. M. Sheldrick *Acta Crystallogr. Sect A Found Adv.*, 2015, **A71**, 3.
- 3 G. M. Sheldrick. *Acta Crystallogr. Sect C Struct. Chem.*, 2015, **C71**, 3.
- 4 Spek AL. *PLATON: A Multipurpose Crystallographic Tool*; Utrecht University: Utrecht, The Netherlands. 2001.
- 5 A-L Myers and J. M. Prausnitz, *AIChE J.*, 1965, **11**, 121.
- 6 L-B. Li, H.-M. Wen, C. He, R.-B. Lin, R. Krishna, H. Wu, W. Zhou, J. Li, B. Li, B.-L. Chen, *Angew. Chem., Int. Ed.*, 2018, **57**, 15183.
- 7 Y.-B. Wu, C. Xiong, Q.-Y. Liu, J.-G. Ma, F. Luo and Y.-L. Wang, *Inorg. Chem.*, 2021, **60**, 6472.
- 8 Z.-T. Lin, Q.-Y. Liu, L. Yang, C.-T. He, L. Li and Y.-L. Wang, *Inorg. Chem.*, 2020, **59**, 4030.
- 9 Z. Li, L.-Y. Li, L.-D. Guo, J.-W. Wang, Q.-W. Yang, Z.-G. Zhang, Y.-W. Yang, Z.-B. Bao and Q.-L. Ren, *Ind. Eng. Chem. Res.*, 2020, **59**, 13716.
- 10 T. Ke, Q.-J. Wang, J. Shen, J.-Y. Zhou, Z.-B. Bao, Q.-W. Yang and Q.-L. Ren, *Angew. Chem. Int. Ed.*, 2020, **59**, 12725.
- 11 L.-F. Yang, X.-L. Cui, Z.-Q. Zhang, Q.-W. Yang, Z.-B. Bao, Q.-L. Ren and H.-B. Xing, *Angew. Chem., Int. Ed.*, 2018, **57**, 13145.
- 12 Y. Peng, C. He, T. Pham, T. Wang, P. Li, R. Krishna, K. A. Forrest, A. Hogan, S. Suepaul, B. Space, M. Fang, Y. Chen, M. J. Zaworotko, J. Li, L. Li, Z. Zhang, P. Cheng and B. Chen, *Angew. Chem. Int. Ed.*, 2019, **58**, 10209.
- 13 L. Li, L. Guo, F. Zhang, Z. Zhang, Q. Yang, Y. Yang, Q. Ren and Z. Bao, *ACS Appl. Mater. Interfaces*, 2020, **12**, 17147.

- 14 L.-F. Yang, X.-L. Cui, Q.-W. Yang, S.-H. Qian, H. Wu, Z.-B. Bao, Z.-G. Zhang, Q.-L. Ren, W. Zhou, B.-L. Chen and H.-B. Xing, *Adv. Mater.*, 2018, **30**, 1705374.
- 15 L. Li, R.-B. Lin, R. Krishna, X. Wang, B. Li, H. Wu, J. Li, W. Zhou and B. Chen, *J. Am. Chem. Soc.*, 2017, **139**, 7733.
- 16 Q.-J. Wang, J.-B. Hu, L.-F. Yang, Z.-Q. Zhang, T. Ke, X.-L. Cui and H.-B. Xing, *Nat. Commun.*, 2022, **13**, 2955.
- 17 Y.-L. Peng, T. Wang, C.-N. Jin, C.-H. Deng, Y.-M. Zhao, W.-S. Liu, K.A. Forrest, R. Krishna, Y. Chen, T. Pham, B. Space, P. Cheng, M.J. Zaworotko and Z.-J. Zhang, *Nat. Commun.*, 2021, **12**, 5768.
- 18 Y.-J. Jiang, J.-B. Hu, L.-Y. Wang, W.-Q. Sun, N. Xu, R. Krishna, S. Duttwyler, X.-L. Cui, H.-B. Xing and Y.-B. Zhang, *Angew. Chem. Int. Ed.*, 2022, **61**, e202200947.
- 19 L.-F. Yang, X.-L. Cui, Y.-B. Zhang, Q.-W. Yang and H.-B. Xing, *J. Mater. Chem. A*, 2018, **6**, 24452.
- 20 G.-X. Jin, T. Wang, T.-X. Yue, X.-K. Wang, F.-N. Dai, X.-W. Wu, Q.-K. Liu and J.-P. Ma, *Chem. Commun.*, 2021, **57**, 13325.
- 21 X.-Q. Wu, J.-H. Liu, T. He, P.-D. Zhang, J. Yu and J.-R. Li, *Chem. Eng. J.*, 2021, **407**, 127183.
- 22 Z.-Q. Zhang, Q. Ding, J.-Y. Cui, X.-L. Cui and H.-B. Xing, *Small*, 2020, **16**, 2005360.
- 23 Y. Peng, T. Wang, C. Jin, P. Li, S. Suepaul, G. Beemer, Y. Chen, R. Krishna, P. Cheng, T. Pham, B. Space, M. Zaworotko and Z.-J. Zhang, *J. Mater. Chem. A*, 2021, **9**, 2850.
- 24 S.-X. Zou, Z.-Y. Di, H. Li, Y.-Z. Liu, Z.-Y. Ji, H.-B. Li, C. Chen, M.-Y. Wu and M.-C. Hong, *Inorg. Chem.*, 2022, **61**, 7530.
- 25 M.-M. Xu, Y.-H. Liu, X. Zhang, H.-T. Wang, L.-H. Xie and J.-R. Li, *Inorg. Chem. Front.*, 2022, **9**, 4952.
- 26 X.-Q. Wu, Y. Xie, J.-H. Liu, T. He, Y.-Z. Zhang, J. Yu, X.-J. Kong and J.-R. Li, *J. Mater. Chem. A*, 2019, **7**, 25254.